THE BRIDGING DOMAIN MULTISCALE METHOD AND ITS HIGH PERFORMANCE COMPUTING IMPLEMENTATION

Shaoping Xiao

Department of Mechanical and Industrial Engineering

Center for Computer-Aided Design

The University of Iowa, Iowa City, IA 52242

shaoping-xiao@uiowa.edu

Jun Ni

Department of Radiology

Department of Mechanical Engineering

Department of Computer Science

The University of Iowa, Iowa City, IA 52242

jun-ni@uiowa.edu

Shaowen Wang

CyberInfrastructure and Geospatial Information Laboratory

Department of Geography

National Center for Supercomputing Applications

University of Illinois at Urbana-Champaign, Urbana, IL 61801

shaowen@uiuc.edu

ABSTRACT

This paper presents a study on the feasibility of applying high performance computing (HPC) to the Bridging Domain Multiscale (BDM) method, so that featured scalable multiscale computations can be achieved. Wave propagation in a molecule chain through an entire computational domain is employed as an example to demonstrate its applicability and computing performance when multiscale-based simulations are conducted in a large-scale parallel computing environment. In addition, the conceptual idea and computing framework using Grid computing technologies is proposed to enhance future multiscale computations in nanotechnology.

Keywords: multiscale, bridging domain, high performance computing, Grid computing, nanotechnology

1. Introduction

Nanotechnology is used to create innovative materials with new functional or multifunctional structures and novel devices on a nanometer (10^{-9}m) scale. Nanotechnology has emerged in multidisciplinary research fields. For instance, numerical methods in computational science play a crucial role in the research fields of nano-mechanics and materials science, especially in simulating and understanding the principal design or fabrication of novel nanoscale materials such as nanocomposites. Among these methods, molecular dynamics (MD) is one of the effective and efficient numerical methods that have been widely used in elucidating complex physical phenomena[1-5] on a nanoscale. Although MD has many advantages, it exhibits limitations with respect to both length and time scales. For example, a material with a cubic volume of 1 m^3 contains trillions of atoms, and a typical time-step in MD simulation is roughly one femtosecond (~10^{-15}s). Consequently, these characteristics limit the use of MD for simulation of many physical phenomena, such as material failure problems. At present, a complete MD modeling is unrealistic, especially for completely simulating a material system with heterogeneity, even with powerful high-end computers. Therefore, there exists an urgent need to develop a new and applicable methodology that can be used to efficiently simulate large nanosystems.

Recently, the development of efficient multiscale methods that are capable of addressing large length and time scales has been addressed in computational nanotechnology for the design of novel nanoscale materials and devices[6]. Multiscale methods can be divided into two classes: hierarchical[7-10] and concurrent multiscale methods[11-16]. In hierarchical

methods, the continuum approximation is based on the properties of a subscale model, such as an MD model. The intrinsic properties of the material are determined at the atomic level and embedded in a continuum model using a homogenization procedure. Classical hierarchical multiscale methods include quasicontinuum methods[7] and discontinuous Galerkin (DG) methods within the framework of the Heterogeneous Multiscale Method (HMM)[8]. Most hierarchical methods assume that nanostructures are perfect molecular structures subject to zero temperature. Xiao and Yang[9,10] proposed nanoscale meshfree particle methods with a temperature-related homogenization for nanoscale continuum modeling and simulation.

Concurrent multiscale methods employ an appropriate model in different subdomains to treat each length scale simultaneously. In a pioneering work, Abraham et al.[11,12] developed a methodology called MAAD (Macro-Atomistic-Ab initio-Dynamics) in which a tight-binding quantum mechanical calculation is coupled with MD and, in turn, coupled with a finite element continuum model. Choly et al.[13] presented formalism for coupling a density-functional-theory-based quantum simulation within a classical simulation for the treatment of simple metallic systems. Recently, several concurrent multiscale techniques that couple continuum and molecular models in particular have been developed. Wagner and Liu[14] developed a multiscale method in which the molecular displacements are decomposed into fine scale (molecular) and coarse scale (continuum). Belytschko and Xiao[15,16] coupled MD with continuum mechanics via a bridging domain.

A concurrent multiscale method can be designed to span a range of physical domains of different length scales, from atomic to microscopic/mesoscopic to macroscopic scales. Unfortunately, most multiscale methods still require intensive computation for large nanoscale simulations, although such limitations are much smaller than those associated with full MD simulations. On the other hand, due to the highly intensive computation requirement, a single-processor computer is barely sufficient to handle simulations that typically involve trillions of atoms and up to several seconds. The limitation of computing capacity naturally motivates an alternative approach—to conduct concurrent multiscale computations based on high performance computing (HPC) or Grid-based distributed computing. To date, a few HPC-based multiscale simulations have been reported. For example, Yanovsky[17] utilized parallel computing technologies to study polymer composite properties. Ma et al.[18] implemented their continuum/atomic coupling algorithm in the Structural Adaptive Mesh Refinement Application Infrastructure (SAMRAI) using parallel processing to study two-dimensional crack propagation. However, most existing works do not focus on HPC algorithm development and efficiency.

In the U.S., the Cyberinfrastructure recently promoted by the National Science Foundation (NSF) provides a gateway to future science and engineering discovery. It enables large-scale resource sharing, especially distributed HPC systems with unprecedented computational capacity. Such capacity reaches several hundred teraflops, and upgrading to petaflops is just a few years away on the NSF TeraGrid—a Grid computing environment and key element of U.S. cyberinfrastructure. Grid computing

technologies enable users to assemble large-scale distributed computational resources to create a secured virtual supercomputer that can be used to accomplish a specific purpose[19]. This assemblage of distributed resources is dynamically orchestrated using a set of protocols as well as specialized software referred to as Grid middleware. This coordinated sharing of resources takes place within formal or informal consortia of individuals and/or institutions often referred to as Virtual Organizations (VO)[20]. Grid computing technologies give scientists the ability to handle large-scale computations, especially in nanotechnology investigations.

In this paper, we will develop a scalable, parallel bridge domain coupling algorithm for computations in nanotechnology applications. The bridging domain coupling method is described in Section 2 after the introduction. This coupling method is extended to a scalable parallel multiscale method in Section 3. Associated domain decomposition and communication algorithms are explained, and a one-dimensional example is studied for investigating computing performance. Section 4 offers a description of the feasibility of multiscale modeling and simulation using Grid computing, followed by a conclusion.

2. Bridging domain coupling method

The Bridging Domain Coupling Method (BDCM) was proposed by Xiao and Belytschko[15,16]. Here, we first provide a brief summary of this methodology, detailed in a one-dimensional molecule chain that includes a molecular dynamics domain, a finite

element (continuum) domain, and a bridging domain where the molecular and continuum domains overlap, as shown in Figure 1.

(Figure 1)

Generally, a BDCM method serves as a linkage between molecular and continuum models through an overlapped domain. The continuum domain, Ω^C, modeled by a macroscopic continuum model, overlaps the molecular domain, Ω^M, modeled by a molecular model, through an interaction region, called a bridging domain, Ω^{int}. The superscripts "M" and "C" refer to the molecular and continuum domains, while the superscript "int" refers to the interaction domain or bridging domain where a bridging domain method is applied. In the bridging domain method, the total energy is taken to be a linear combination of the molecular and continuum energies. Therefore, in the bridging domain, the molecular and continuum models co-exist. A linear switch scaling parameter α is introduced hereby in the overlapped bridging domain. For example, the parameter α can be proposed as

$$\alpha = \begin{cases} 0 & in \quad \Omega_0^M - \Omega_0^{int} \\ [0,1] & in \quad \Omega_0^{int} \\ 1 & in \quad \Omega_0^C - \Omega_0^{int} \end{cases} . \qquad (1)$$

The Hamiltonian energy for the complete domain can be considered as a linear combination of the molecular and continuum counterparts. It can be expressed as

$$H = (1-\alpha)H^M + \alpha H^C = \sum_I [1-\alpha(X_I)]\frac{m_I \dot{d}_I^2}{2} + (1-\alpha)W^M + \int_{\Omega_0^C} \frac{1}{2}\alpha\rho_0 v_I^2 d\Omega_0^C + \alpha W^C$$
$$= \frac{1}{2}\sum_I [1-\alpha(X_I)]m_I \dot{d}_I^2 + (1-\alpha)W^M + \frac{1}{2}\int_{\Omega_0^C} \alpha\rho_0 v_I^2 d\Omega_0^C + \alpha W^C \quad (2)$$

where m_I and d_I are the mass and displacement of the atom, ρ_0 is the initial density in the finite element domain, v_I is the velocity of node I, and W^C is the total strain energy in the continuum domain. In the molecular domain, $W^M(x)$ refers to the potential function that is the summation of all energies due to any force field (such as the pair-wise interaction of the atoms, three-body potentials, or others). Assume the potential is due only to a constant external force, $\bar{f}_I^{ext}$, such as electrostatic forces, and a pair-wise interatomic potential is denoted by $w_{IJ} = w_M(x_I, x_J)$, where x is the coordinate. The total potential can be expressed as

$$W^M = -W_M^{ext} + W_M^{int} = -\sum_I \bar{f}_I^{ext} d_I + \sum_{I,J>I} w_M(x_I, x_J). \quad (3)$$

The strain energy of the continuum model is defined by

$$W^C = \int_{\Omega_0} w_C d\Omega \quad (4)$$

where w_C is the potential energy per unit volume within the continuum domain. It depends on the elongations and angle changes of the atomic bonds that underlie the continuum model. The potential energy density can be calculated based on the homogenization techniques[7]. If temperature effects are considered, the free energy density, instead of the potential energy density, is employed in Eq. (4), and calculation can be performed based on the temperature-related Cauchy-Born rule[9,10].

In the bridging domain, a Lagrange multiplier can be used to conjunct the molecular and the continuum domains, with the following constraints: $u(X_I,t)-d_I(t)=0$, where $u(X_I,t)=\sum_J N_J(X_I)u_J$ is the finite element interpolated displacement of atom I. The total Hamiltonian energy of the system can then be expressed as

$$H=(1-\alpha)H^M+\alpha H^C+\sum_{I\in\Omega^{\text{int}}}\lambda(X_I)\left(u^C(X_I,t)-u_I^M(t)\right). \tag{5}$$

Based on Hamiltonian mechanics, the following discrete equations can be derived:

$$\begin{aligned} \overline{M}_I\ddot{u}_I &= f_I^{extC}-f_I^{intC}-f_I^{LC} && in \quad \Omega_0^C \\ \overline{m}_I\ddot{d}_I &= f_I^{ext}-f_I^{int}-f_I^{L} && in \quad \Omega_0^M \end{aligned} \tag{6}$$

where

$$\overline{M}_I=\alpha(X_I)M_I \qquad \overline{m}_I=(1-\alpha(X_I))m_I$$

and M_I is the nodal mass associated with node I.

The external nodal forces, including the scaling factor, are defined as

$$\begin{aligned} f_I^{extC} &= \int_{\Omega_0^C}\alpha(X)N_I\rho_0 b\,d\Omega_0^C+\int_{\Gamma_0^t}\alpha(X)N_I\bar{t}\,d\Gamma_0^t \\ f_I^{ext} &= (1-\alpha(X_I))\bar{f}_I^{ext} \end{aligned} \tag{7}$$

where b is the body force per unit mass and $\bar{t}$ is the traction applied on the boundary Γ_0 in the continuum domain.

Similarly, the internal forces are

$$f_I^{intC} = \int_{\Omega_0^C} \alpha(X)\rho_0 \frac{\partial w_C(F)}{\partial u_I} d\Omega_0^C \tag{8}$$

$$f_I^{int} = (1-\alpha(X_I)) \sum_{I,J>I} \frac{\partial w_M(x_I, x_J)}{\partial d_I}. \tag{9}$$

The forces f_I^{LC} and f_I^{L} are due to the constraints enforced by the Lagrange multipliers, and they are

$$\begin{aligned} \mathrm{f}_\mathrm{I}^{\mathrm{LC}} &= \sum_{\mathrm{J}} \lambda_\mathrm{J} \frac{\partial \mathrm{g}_\mathrm{J}}{\partial \mathrm{u}_\mathrm{I}} = \sum_{\mathrm{J}} \lambda_\mathrm{J} \mathrm{N}_\mathrm{J}(\mathrm{X}_\mathrm{I}) \\ \mathrm{f}_\mathrm{I}^{\mathrm{L}} &= \sum_{\mathrm{J}} \lambda_\mathrm{J} \frac{\partial \mathrm{g}_\mathrm{J}}{\partial \mathrm{d}_\mathrm{I}} = \sum_{\mathrm{J}} \left(-\lambda_\mathrm{J} \delta_{\mathrm{IJ}}\right). \end{aligned} \tag{10}$$

An explicit algorithm to solve the above discrete equations is described below:

1. Initialize the domains, displacements, velocities, and accelerations
2. Calculate the trail displacements with constraints neglected:

$$\begin{aligned} u^*_{I(n+1)} &= u_{I(n)} + \dot{u}_{I(n)}\Delta t + \frac{1}{2}\ddot{u}_{I(n)}\Delta t^2 \qquad in \quad \Omega_0^C \\ d^*_{I(n+1)} &= d_{I(n)} + \dot{d}_{I(n)}\Delta t + \frac{1}{2}\ddot{d}_{I(n)}\Delta t^2 \qquad in \quad \Omega_0^M \end{aligned} \tag{11}$$

(The subscripts in parentheses are the time step numbers). In the equations above, the accelerations are obtained from Eq. (6) without considering the forces due to the constraints; therefore,

$$\begin{aligned} \ddot{u}^*_{I(n+1)} &= \frac{1}{\overline{M}_I}\left[f^{extC}_{I(n+1)} - f^{\mathrm{int}\,C}_{I(n+1)}\right] \qquad in \quad \Omega_0^C \\ \ddot{u}^*_{I(n+1)} &= \frac{1}{\overline{m}_I}\left[f^{ext}_{I(n+1)} - f^{\mathrm{int}}_{I(n+1)}\right] \qquad in \quad \Omega_0^M \end{aligned} \tag{12}$$

3. Calculate the trial velocities:

$$\dot{u}^*_{I(n+1)} = \dot{u}_{I(n)} + \frac{1}{2}\left[\ddot{u}_{I(n)} + \ddot{u}_{I(n+1)}\right]\Delta t \quad in \quad \Omega_0^C$$
$$\dot{d}^*_{I(n+1)} = \dot{d}_{I(n)} + \frac{1}{2}\left[\ddot{d}_{I(n)} + \ddot{d}_{I(n+1)}\right]\Delta t \quad in \quad \Omega_0^M \tag{13}$$

4. Compute unknown Lagrange multipliers:

$$\sum_L A_{IL}\lambda_L = g^*_I = \sum_J N_J(X_I)\dot{u}^*_J - \dot{d}^*_I \tag{14}$$

where

$$A_{IL} = \Delta t \overline{M}_I^{-1}\sum_J N_J(X_I)N_L(X_J) - \Delta t \overline{m}_I^{-1}\delta_{LI}$$

5. Update the velocities:

$$\dot{u}_{I(n+1)} = \dot{u}^*_{I(n+1)} - \overline{M}_I^{-1}\Delta t\sum_J N_J(X_I)\lambda_J \tag{15}$$

$$\dot{d}_{I(n+1)} = \dot{d}^*_{I(n+1)} - \overline{m}_I^{-1}\Delta t\sum_J(-\delta_{IJ})\lambda_J \tag{16}$$

6. Repeat Step 2 through Step 5 until the end of simulation.

As an example, we simulate wave propagation in a one-dimensional molecule chain, which contains 431 atoms. The Lennard-Jones (LJ) 6-12 potential is employed to describe the inter-atomic interaction between two neighboring atoms. This potential is expressed as

$$W^M(r_{ij}) = 4\varepsilon\left[\left(\frac{\sigma}{r_{ij}}\right)^{12} - \left(\frac{\sigma}{r_{ij}}\right)^{6}\right] \tag{17}$$

where the parameters are $\varepsilon = 0.2J$ and $\sigma = 0.11nm$. The equilibrium bond length is given as $r_0 = 0.139nm$.

In the bridging domain coupling model of the molecule chain similar to that in Figure 1, the molecular domain contains 211 atoms, and there are 40 elements of equal length in the continuum domain., Each element contains approximately 5 atoms. The bridging domain includes 6 finite elements. In the continuum model, all the bonds in a single element are assumed to be deformed uniformly. Consequently, the length of deformed bonds in this single element is $r = Fr_0$, where F is the deformation gradient in this element. In computing the nodal internal forces via Eq. (8), the strain energy density in an element is the potential energy density:

$$w_C(F) = \frac{4\varepsilon}{r_0}\left[\left(\frac{\sigma}{Fr_0}\right)^{12} - \left(\frac{\sigma}{Fr_0}\right)^{6}\right]. \tag{18}$$

During the simulation, the time step is 0.002 ps. There are initial displacements on the atoms in the left portion of the molecular domain. The initial displacements contain a combination of high-frequency and low-frequency modes. Once the simulation starts, there is a wave propagating from the molecular domain to the continuum domain. Since the length of the high-frequency wave is larger than the element length in the continuum domain, a nonphysical wave reflection phenomenon may occur in most multiscale simulations[16]. However, the bridging domain coupling technique can automatically eliminate such a phenomenon, as shown in Figure 2.

(Figure 2)

3. Bridging domain multiscale method with parallel computing

3.1 Bridging domain multiscale method

(Figure 3)

The bridging domain coupling method can be extended for coupling the nanoscale to the microscale and macroscale for a given system, as shown in Figure 3. A macroscale domain (~10^{-3} m) can be modeled as a linear elasticity domain using finite element methods[21]. The elastic properties are obtained using a Representative Volume Element (RVE) model from an MD simulation at a given temperature. A microscale domain (~10^{6}m) can be embedded in the macroscale domain, modeled using a nonlinear FE method[22]. The homogenization techniques, such as the TCB rule[9,10], can be implemented in the nonlinear FE method to construct the temperature-dependent constitutive equations of the continuum. A subdomain in the microscale domain can be treated as a nanoscale (molecular) domain (~10^{-9} m) using MD if one is interested in studying physical phenomena in this subdomain. We can employ a Hoover thermostat[23] to maintain the nanoscale domain at a given temperature. It should be noted that a number of different length scales, such as the mesoscale domain, could be added as desired between the macroscale and microscale continuum domains. Furthermore, even the macroscale or the microscale can contain a number of different length scale subdomains. Different length scales are coupled via the bridging domain coupling technique[16].

Most concurrent multiscale methods employ multiple length scales but only a single time step. In coupling finite element methods and molecular dynamics, if the finite element mesh is graded down to the atomic spacing at the interface of the continuum and molecular domains[11], the time step must be restricted to the order of one femtosecond (10^{-15} s), due to the stability requirement in the molecular model. Consequently, significant computation time is wasted for large length scales in which large time steps can be used. In the bridging domain multiscale method, coupling different scales without such grading down of mesh sizes will be achieved by a straightforward implementation of different time steps via a multiple-time-step algorithm.

(Figure 4)

Since uniform meshes can be used in each length scale in the bridging domain multiscale method, it is possible to apply different time steps in different length scales, as shown in Figure 4. A multiple-time-step algorithm is proposed for the bridging domain multiscale method. For example, to couple a molecular model at the nanoscale and a continuum model at the microscale, a fine time step, $\Delta\tau$, is used in the molecular model and a coarse time step, $\Delta t = N\Delta\tau$, is used in the microscopic continuum model. Eq. (13) is then rewritten as:

$$\begin{aligned} \dot{u}^{*}_{I(n+1)} &= \dot{u}_{I(n)} + \frac{1}{2}\left[\ddot{u}_{I(n)} + \ddot{u}_{I(n+1)}\right]\Delta t \qquad in \quad \Omega_0^C \\ \dot{d}^{*}_{I(n+\frac{j+1}{N})} &= \dot{d}_{I(n+\frac{j}{N})} + \frac{1}{2}\left[\ddot{d}_{I(n+\frac{j}{N})} + \ddot{d}_{I(n+\frac{j+1}{N})}\right]\Delta\tau \qquad in \quad \Omega_0^M \end{aligned} \tag{19}$$

The bridging domain then connects a fine length/time scale and a coarse length/time scale. Compatibility of different length scales will be enforced by means of a constraint imposed via the Lagrange multiplier method, i.e., Eq. (14), at each coarse time step, Δt, as shown in Figure 4. Consequently, the equations of motion will be solved independently in different length scales with different time steps. At each coarse time step, velocities of nodes/atoms in the bridging domain will be corrected via the bridging domain coupling technique.

3.2 Domain Decomposition

(Figure 5)

To perform such multiscale simulations via high performance computing, efficient and effective domain decomposition strategies are necessary. In the bridging domain multiscale method, as illustrated in Figure 5, a simulation domain can be easily hierarchically divided into subdomains, each of which can be processed in parallel.

1) The entire domain is divided into several sub-domains based on the scale difference. The primarily decomposed sub-domains are called the first-generation (FG) subdomains. The computational jobs on the subdomains can be distributed to different groups of HPC processors. For example, the computations in the molecular domain can be performed at Group 1 (a group of processors within a single HPC cluster), while those in the microscale/macroscopic domains can be performed at Group 2 (another group of

processors within a single HPC cluster). The first-generation subdomain decomposition is parallel computing task decomposition. Each FG subdomain is further divided into a number of second-generation (SG) subdomains. Each SG subdomain is assigned to a single processor. In other words, as the secondary effort, the data within the subdomain are decomposed and transferred to each processor within a specified group for intensive computation. Obviously, it is a data-decomposition. This way, the task and data decomposition are combined.

2) A bridging subdomain is a special subdomain. It is shared by two SG subdomains, each of which belongs to two different length scales. Although one SG subdomain can overlap more than one other SG subdomain, the bridging subdomains do not overlap each other.

3) Inter-domain communications between two SG subdomains take place in each FG subdomain separately. Such inter-domain communications occur prior to solution of the equations of motion so that the motion of atoms or nodes at the SG subdomain boundaries is consistent.

4) The procedure for solving equations of motion in each FG subdomain is independent.

5) Once the equations of motion are solved at each time step (or coarse time step in the event that a multiple-time-step algorithm is used), the bridging domain communications take place between two processors. It should be noted that those two processors belong to two different groups of processors, shown in Figure 4. The bridging coupling techniques are applied to correct the trial velocities of nodes or atoms in each bridging subdomain independently.

3.3 Inter-domain and bridging domain communications

Figure 6 illustrates the inter-domain communication in the BDM method. A simple BDM model contains two subdomains, Ω_A and Ω_B, in the molecular domain and two subdomains, Ω_C and Ω_D, in the continuum domain. Ω_A and Ω_B are allocated to two different processors in the same group of processors. Similarly, Ω_C and Ω_D are allocated to two processors in another group of processors. Inter-domain communications occur between Ω_A and Ω_B or between Ω_C and Ω_D prior to solution of the equations of motion. Such communications take place only inside each group of processors. In the molecular domain, Ω_A and Ω_B share atom E. Since the multi-body potential functions are generally utilized in MD simulations, slave domains Ω_B^{int} and Ω_A^{int}, associated with Ω_A and Ω_B, respectively, are introduced to support energy and force calculations. For example, the motion of atom H is updated in Ω_B. Such information is passed to the slave domain Ω_B^{int} to assist in the calculation of the interatomic force of atom E in Ω_A because the potential in the molecular domain includes the angle-bending potential of bonds GE and HE. Similarly, the motion of atom G is updated in Ω_A. Such information is passed to the slave domain Ω_A^{int} to assist in the calculation of the interatomic force of atom E in Ω_B. Consequently, after solving the equations of motion, the updated motions of atom E in either subdomain Ω_A or Ω_B are identical to avoid the occurrence of nonphysical phenomena. It should be noted that the size of a slave domain depends on the selected potential functions, in particular the cutoff distance for Van der Waals potential functions.

(Figure 6)

The inter-domain communication in the continuum domain has a different strategy from the one in the molecular domain. The continuum subdomains Ω_C and Ω_D share the boundary node F, as shown in Figure 6. F^C and F^D are used to represent the same node F, but in different subdomains. Unlike inter-domain communication between neighboring molecular subdomains, inter-domain communication between neighboring continuum subdomains does not require slave domains, instead acting to aid the exchange of calculated internal forces of boundary nodes. For instance, the internal force of node F^C, calculated in subdomain Ω_C, is passed to subdomain Ω_D and is set as the negatively external force of node F^D. A similar procedure is performed to pass the internal force of node F^D, calculated in subdomain Ω_D, to subdomain Ω_C as the negatively external force of node F^C. Therefore, the motions of node F, updated by solving the equations of motion, Eq. (6), in both subdomains Ω_C and Ω_D, are identical.

(Figure 7)

Once the equations of motion are solved independently in each processor, the bridging-domain communication occurs separately in each bridging subdomain, e.g., Ω_{AC}^{B} and Ω_{BD}^{B} in Figure 7. For example, trial velocities of atoms in Ω_{BD}^{B} of Ω_B are passed to Ω_D, while trial velocities of nodes in Ω_{BD}^{B} of Ω_D are passed to Ω_B. Then, the Lagrange multipliers in Ω_{BD}^{B} are solved via Eq. (14). Last of all, the trial velocities of atoms and

nodes in the bridging domain Ω_{BD}^{B} will be corrected in Ω_B and Ω_D, independently through Eqs. (15) and (16).

Upon the above domain decomposition and data communication, the parallel computing processing can be implemented in the workflow illustrated in Figure 8.

(Figure 8)

3.4 Complexity and performance evaluations

An important focus of the proposed method is the definition of a suitable computational intensity metric for sub-domains:

$$M(d) = f(D(d), \boldsymbol{O}, P) \tag{20}$$

where M is a function of the domain size D, i.e., the number of nodes or atoms having sub-domain d, the computing time complexity $\boldsymbol{O}$ of a particular component of a multiscale method, and parameters P that characterize the computing capacity of each specific HPC resource. M will be used to determine the size of sub-domains in domain decomposition. M is also an important parameter that can be used to guide decisions about when and where these sub-domains should be scheduled.

The computing time complexity of a continuum domain is $\boldsymbol{O}(n^2)$ while the complexity for a molecular domain is $\boldsymbol{O}(m^2)$, where m represents the number of atoms and n the number of finite element nodes. Although the complexity representation is the same for these two domains, m is often significantly larger than n. $\boldsymbol{O}(m^2)$ is approximately within the

range $\boldsymbol{O}(n^3)$ to $\boldsymbol{O}(n^4)$, because m is approximately equivalent to $n^{3/2\sim2}$. The domain decomposition approach will address this complexity difference to produce sub-domains adaptively, the representations of which include the complexity information for tasking scheduling purposes. This approach will help detach the domain decomposition technique from the task-scheduling advisor, as described in the following. Further research will be conducted for multiple time steps as used in different length scales.

In order to investigate the feasibility, reliability, and application of the proposed method, several high performance computing benchmark studies should be conducted. The studies include (1) parallel performance speedup and efficiency to evaluate the behavior of high-performance computing, (2) detailed data communication (blocking, non-blocking, gather/scatter, one-site-communication effect using MPI2 features, parallel I/O, network impacts and network latency, load balance, etc.) among a group of processors and computational nodes to understand and reduce the communication loss, and (3) experiments of different HPC platforms and an analytical model of HPC scalability.

3.5 One-dimensional examples

To demonstrate the preliminary feasibility of the bridging domain multiscale method with high performance computing techniques, an experimental model has been developed. Similar to the previous example, the experiment is designed to observe the propagation of an imposed wave in a molecule chain passing from the molecular domain to the continuum domain. In this example, the bridging domain multiscale model contains 10,000 atoms and 10,000 finite elements. Each finite element contains 9 atoms.

Therefore, the molecule chain has 100,000 atoms, and the length of the chain is around 20 micrometers. In this example, we mainly study the speedup of simulations due to high performance computing. The first computation is conducted on a local cluster (Microway 64-bit AMD Opeteron 32 processors). Figure 9(a) presents the speedup performance. The parallel performance increase exhibits a quasi-linear behavior. In order to test the parallel scalability, we also employed the algorithm on NSF's TeraGrid (NCSA) system with 100 processors. The computational results are very promising, as shown in Figure 9(b). Due to the large memory required for the finite element method, a superlinear behavior is observed. The preliminary study successfully demonstrates the feasibility and applicability of the proposed model. The achieved computations provide significant experience for future multi-dimensional studies.

(Figure 9)

4. Grid computing techniques in multiscale simulations

4.1 Nano-middleware

During the last several years, Computational Grids have been widely used to address computationally intensive problems in science, engineering, and commerce[24,25]. Several disciplines have employed Grid computing to obtain solutions to computationally intensive problems by developing domain-specific middleware. This domain-specific middleware exploits characteristics of domain problems and aids the efficient use of Grids. In a similar manner, Grid application-specific middleware must be developed for multiscale methods to capture important method characteristics. This paper develops a

conceptual framework for multiscale methods that supports the location, allocation, and utilization of Grid resources to effectively and efficiently apply multiscale methods for nanotechnology applications. This middleware is referred to as *nano-middleware* in this paper.

(Figure 10)

The nano-middleware will be designed, as shown in Figure 10, to enable Grid computing of the bridging domain multiscale method. For a given problem, the nano-middleware will schedule decomposed domains to appropriate Grid resources (e.g., clusters) to achieve load balancing and efficient use of resources. The primary components of the nano-middleware are:

1) A task-scheduling advisor that takes the result of domain decomposition as input to produce scheduling plans and achieve high-performance simulation through load-balancing;
2) An information broker (IB) that leverages Grid information services to provide resource discovery[26,27] functions to the task-scheduling advisor;
3) A data access module (DAM) that will manage the transfer, replication, and manipulation of data on the Grid.

Components 1 and 2 primarily deal with computing strategies. Data handling will be supported by existing generic middleware. The task-scheduling advisor is the key

element of nano-middleware for its impact on performance gains. It should be noted that the concept of proposed nano-middleware can be applied to other multiscale methods.

4.2 Task scheduling advisor

Task scheduling is used to schedule subdomains to an appropriate set of Grid resources to achieve optimal performance—tasks are allocated in a way that balances computation across the selection of available resources. In the nano-middleware task-scheduling advisor, subdomains from the computational domain decomposition process are converted to tasks that are then placed in Grid resource queues in a specific order. In practice, queues will be managed by local resource schedulers, such as Portable Batch Systems (PBS) and Condor. The task-scheduling advisor is designed to achieve optimal performance by balancing tasks across available resources[28]. The advisor generates a scheduling plan that determines the correspondence between tasks and the available Grid resources to which they are submitted.

There are two general approaches to task scheduling: static and dynamic. When a static scheduling strategy is employed, the scheduling plan does not change until all tasks are completed[29]. In contrast, dynamic scheduling permits a plan to be altered while the set of tasks is being executed[30]. Using dynamic task scheduling for the BDM method is difficult to accomplish for two specific reasons[31]. First, the computation required to implement dynamic scheduling is much greater than for static scheduling; dynamic scheduling introduces additional overhead penalties created by network latency and the execution of the code that monitors the task status. Also, tasks are swapped between

resources according to a dynamic performance evaluation. Second, fine granularity in individual subdomains, produced based on the BDM method, is desirable in order to achieve high levels of parallelism. Results for these subdomains can be inexpensive to compute even if scheduled to a Grid resource having a small capacity. Therefore, the time overhead that results from implementing dynamic scheduling on a task level may exceed the time required to compute results for an individual subdomain.

Consequently, static scheduling strategies are developed to assign tasks based on computational intensity information for each subdomain, as well as the variability in the computing capacity of each Grid resource. Two principles are used to guide the development of static scheduling algorithms: (1) Grid resources with greater computing capacity are used before those with less capacity; and (2) tasks that are more (less) computationally intensive are assigned to Grid resources with more (less) computing capacity[32].

5. Conclusions

Multiscale modeling and simulation has been at the forefront of nanotechnology research due to its ability to simulate larger systems than is possible with molecular dynamics. In this paper, we first introduced the bridging domain coupling method, which can efficiently couple molecular dynamics and the finite element method. A more powerful multiscale method can be extended to bridge a number of length and time scales via the bridging domain coupling technique.

Recently developed multiscale methods, including the bridging domain multiscale method, still have limitations in length and time scales. This paper proposed an alternative solution for the above problem: high performance computing techniques including Grid computing techniques. The speedup study demonstrated the advantage of implementing high performance computing techniques into the bridging domain multiscale method. Furthermore, the conceptual idea of Grid-based multiscale modeling and simulation will benefit from rapidly developing computer science technologies. Finally, the proposed research in this paper can also be viewed as a framework for implementing high performance computing techniques in other potential multiscale methods.

ACKNOWLEDGEMENTS

We acknowledge support from the Army Research Office (Contract: # W911NF-07-C-0062) and the National Science Foundation (Grant # 0630153 and Grant # 0727007).

REFERENCES:

1. S. Xiao and W. Hou, Phys. Rev. B 73, 115406 (2006)
2. S. Xiao, D. R. Andersen, R. Han and W. Hou, J Comput. Theor. Nanosci. 3, 142 (2006)
3. T. Belytschko, S. Xiao, G. Schatz, R. Ruoff, Phys. Rev. B 65, 235430 (2002)
4. J. S. Smith, D. Bedrov and G. D. Smith, Comp. Sci. Tech. 63, 1599 (2003)
5. C. L. Rountree, R. K. Kalia, E. Lidorikis, A. Nakano, B. L. Van and P. Vashishta, Ann. Rev. Mater. Res. 32, 377 (2002)

6. S. Xiao and W. Hou, Phys. Rev. B 75, 125414 (2007)
7. E. B. Tadmor, M. Ortiz and R. Phillips, Phil. Mag. A 73, 1529 (1996)
8. S. Q. Chen, W. N. E and C. W. Shu, Mult. Model. Simul. 3, 871 (2005)
9. S. Xiao and W. Yang, Int. J. Numer. Meth. Engrg. 69, 2099 (2007)
10. S. Xiao and W. Yang, Comp. Mater. Sci. 37, 374 (2006)
11. F. Abraham, J. Broughton, N. Bernstein and E. Kaxiras, Europhy. Lett. 44, 783 (1998)
12. J. Broughton, F. Abraham, N. Bernstein and E. Kaxiras, Phys. Rev. B 60, 2391 (1999)
13. N. Choly, G. Lu, W. E and E. Kaxiras, Phys. Rev. B 71, 094101 (2005)
14. G. J. Wagner and W. K. Liu, J. Comp. Phys. 190, 249 (2003)
15. T. Belytschko and S. P. Xiao, Int. J. Multi. Comp. Engrg. 1, 115 (2003)
16. S. P. Xiao and T. Belytschko, Comp. Meth. Appl. Mech. Engrg. 193, 1645 (2004)
17. Y. G. Yanovsky, Int. J. Multi. Comp. Engrg. 3, 199 (2005)
18. J. Ma, H. Lu, B. Wang, R. Hornung, A. Wissink, and R. Komanduri, Comp. Model. Engrg. Sci. 14, 101 (2006)
19. I. Foster and C. Kesselman, *The Grid: Blue Print for a New Computing Infrastructure*. Morgan Kaufmann Publishers, Inc. San Francisco, CA, 1999
20. I. Foster, C. Kesselman and S. Tuecke, Int. J. Supercomp. Appl. 15, (2001)
21. T. J. R. Hughes, *The Finite Element Method: Linear Static and Dynamic Analysis,* Prentice-Hall, Dover, 1987.
22. T. Belytschko, W. K. Liu and B. Moran, *Nonlinear Finite Elements for Continua and Structures*, Wiley, New York, 2000
23. W. G. Hoover, Phys. Rev. A 31, 1695 (1985)
24. I. Foster, Phys. Today 55, 42 (2002)

25. F. Berman, G. Fox and T. Hey, "The Grid, past, present, future," In *Grid Computing, Making the Global Infrastructure a Reality*, edited by R. Berman, G. Fox, and T. Hey John Wiley & Sons, West Sussex, England, 2003
26. S. Wang, A. Padmanabhan, Y. Liu, R. Briggs, J. Ni, T. He, B. M. Knosp, Y. Onel, Lec. Note. Comp. Sci. 3032, 536 (2003)
27. Padmanabhan, A., Wang, S., Ghosh, S., and Briggs, R. Proceedings of the Grid 2005 Workshop, Seattle, WA, November 13-14, 2005, IEEE press, pp. 312-317.
28. J. Henrichs, Proceedings of International Conference on Supercomputing 1998, 165 (1998)
29. T. D. Braun, H. J. Siegel, N. Beck, L. L. Boloni, M. Maheswaran, A. I. Reuther, J. P. Robertson, M. D. Theys, B. Yao, D. Hensgen and R. F. Freund, J. Para. Distrib. Comp. 61, 810 (2001)
30. O. Beaumont, A. Legrand and Y. Robert, Para. Comp. 29, 1121 (2003)
31. H. J. Siegel and S. Ali, Euromicro J. Sys. Arch. 46, 627 (2000)
32. S. Wang and M. P. Armstrong, Para. Comp. 29, 1481 (2003)

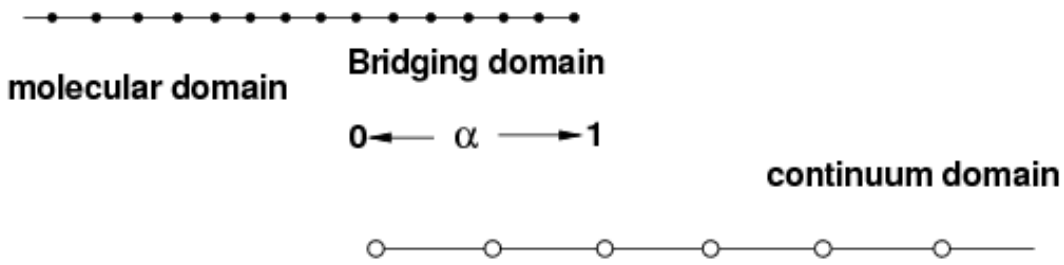

Figure 1. Bridging domain coupling model of a molecule chain

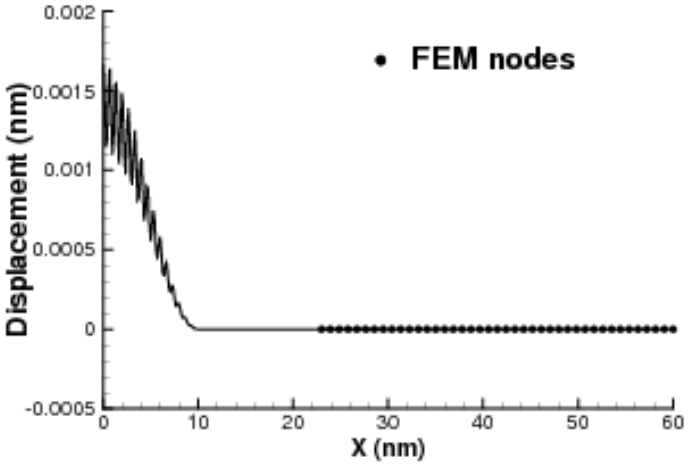

(a)

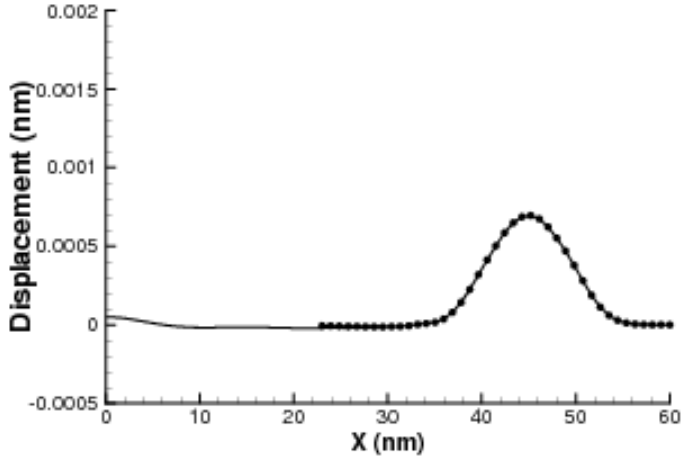

(b)

Figure 2. Wave propagation in 1D molecule chain: (a) Initial wave; (b) Wave propagation

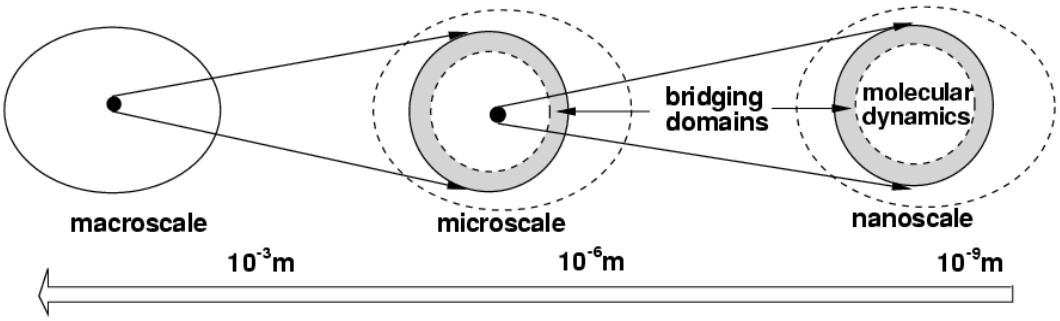

Figure 3. A bridging domain multiscale (BDM) method with different length scales

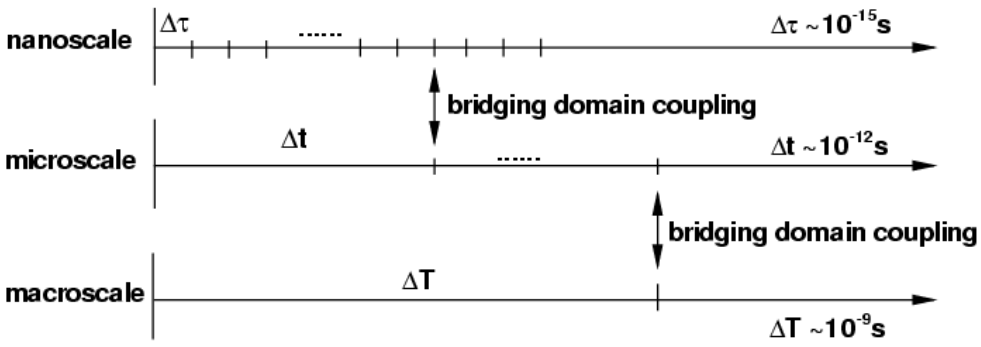

Figure 4. Multiple time steps used in the proposed multiscale method

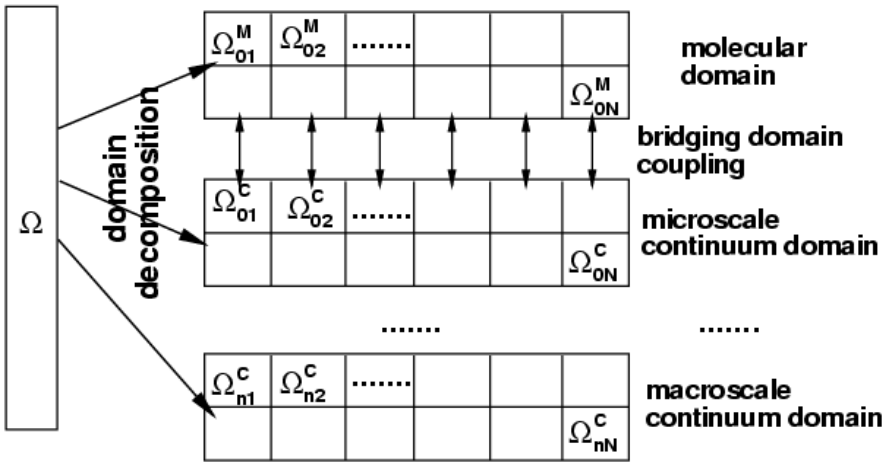

Figure 5. Domain decomposition for the BDM method

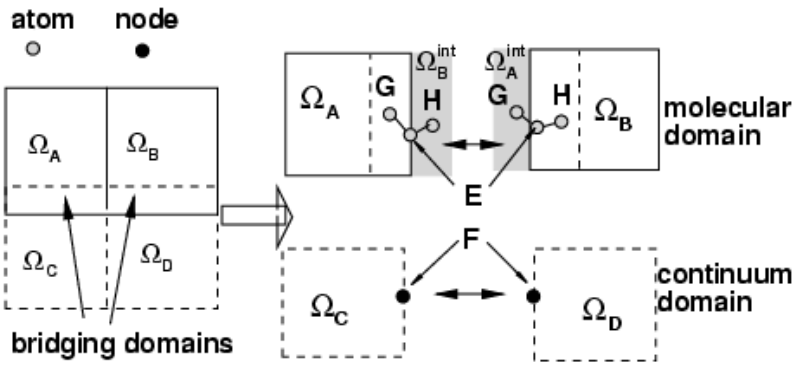

Figure 6. The inter-domain communication

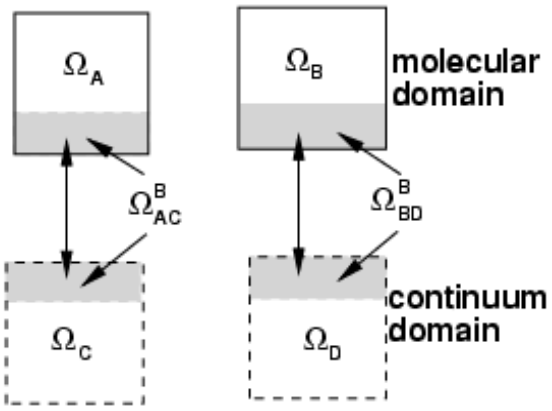

Figure 7. The bridging domain communication

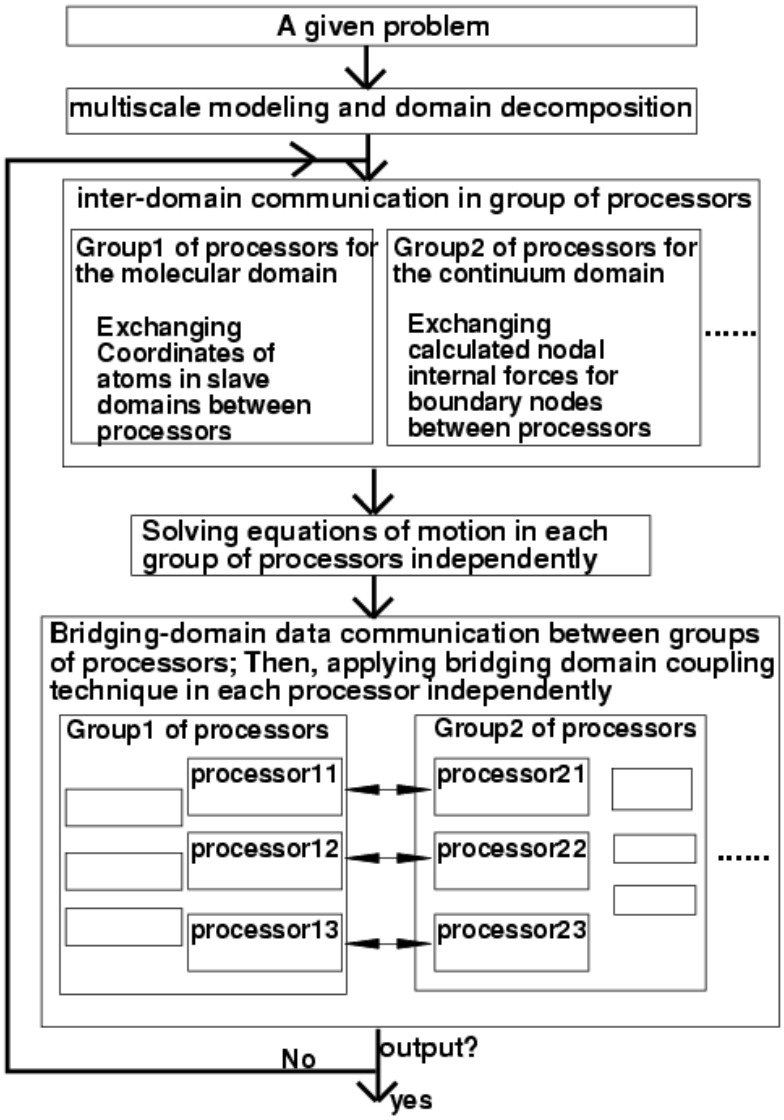

Figure 8. The workflow of the BDM method

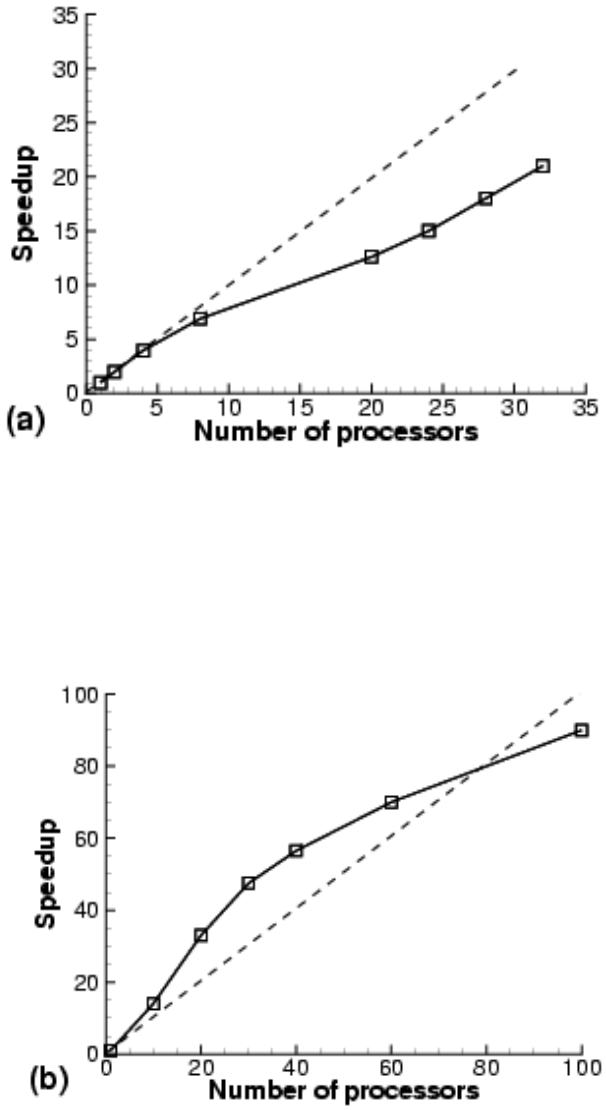

Figure 9. Speedup of 1D BDM method with high-performance computing; (a) on a 32-node UI-IA32-HPC cluster with low memory; and (b) on 64-node NCSA-HPC cluster with larger memory

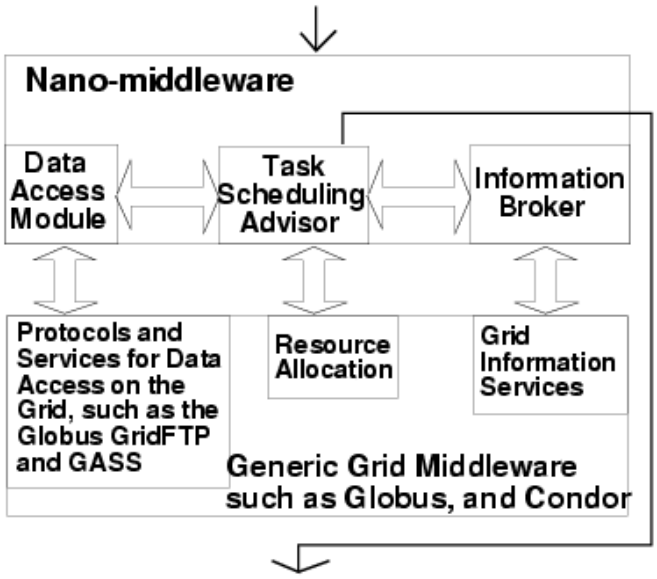

Figure 10. The proposed nano-middleware architecture. **Note:** Globus is a software project, the purpose of which is to develop protocols and services for computational grids. Condor is a high throughput computing system.